4-9-2014

Little Late Holocene Strain Accumulation and Release on the Aleutian Megathrust Below the Shumagin Islands, Alaska

Robert C. Witter

Richard W. Briggs

Simon E. Engelhart
University of Rhode Island, engelhart@mail.uri.edu

Guy Gelfenbaum

Richard D. Koehler

See next page for additional authors

Citation/Publisher Attribution

Witter, R.C.; Briggs, R.W.; Engelhart, S.E.; Gelfenbaum, G.; Koehler, R.D.; Barnhart, W.D. 2014. "Little late Holocene strain accumulation and release on the Aleutian megathrust below the Shumagin Islands, Alaska." Geophysical Research Letters. 41(7): 2359-67. Available at: http://dx.doi.org/10.1002/2014GL059393

Little Late Holocene Strain Accumulation and Release on the Aleutian Megathrust Below the Shumagin Islands, Alaska

Authors

Robert C. Witter, Richard W. Briggs, Simon E. Engelhart, Guy Gelfenbaum, Richard D. Koehler, and William D. Barnhart

AGU PUBLICATIONS

Geophysical Research Letters

RESEARCH LETTER
10.1002/2014GL059393

Key Points:
- Simeonof Island lacks evidence for great earthquakes and tsunamis
- Slow sea-level rise since ~3.4 ka was unperturbed by sudden tectonic jerks
- Creeping subduction in the Shumagin gap probably persisted in the late Holocene

Supporting Information:
- Readme
- Figure S1
- Figure S2
- Figure S3
- Figure S4
- Figure S5
- Figure S6
- Figure S7
- Figure S8
- Figure S9
- Table S1
- Table S2
- Table S3
- Text S1
- Text S2
- Text S3

Correspondence to:
R. C. Witter,
rwitter@usgs.gov

Citation:
Witter, R. C., R. W. Briggs, S. E. Engelhart, G. Gelfenbaum, R. D. Koehler, and W. D. Barnhart (2014), Little late Holocene strain accumulation and release on the Aleutian megathrust below the Shumagin Islands, Alaska, *Geophys. Res. Lett.*, *41*, 2359–2367, doi:10.1002/2014GL059393.

Received 23 JAN 2014
Accepted 24 MAR 2014
Accepted article online 27 MAR 2014
Published online 9 APR 2014

Little late Holocene strain accumulation and release on the Aleutian megathrust below the Shumagin Islands, Alaska

Robert C. Witter[1], Richard W. Briggs[2], Simon E. Engelhart[3], Guy Gelfenbaum[4], Richard D. Koehler[5], and William D. Barnhart[2]

[1]Alaska Science Center, U.S. Geological Survey, Anchorage, Alaska, USA, [2]Geologic Hazards Science Center, U.S. Geological Survey, Golden, Colorado, USA, [3]Department of Geosciences, University of Rhode Island, Kingston, Rhode Island, USA, [4]Pacific Coastal and Marine Science Center, U.S. Geological Survey, Santa Cruz, California, USA, [5]State of Alaska, Division of Geological and Geophysical Surveys, Fairbanks, Alaska, USA

Abstract Can a predominantly creeping segment of a subduction zone generate a great ($M > 8$) earthquake? Despite Russian accounts of strong shaking and high tsunamis in 1788, geodetic observations above the Aleutian megathrust indicate creeping subduction across the Shumagin Islands segment, a well-known seismic gap. Seeking evidence for prehistoric great earthquakes, we investigated Simeonof Island, the archipelago's easternmost island, and found no evidence for uplifted marine terraces or subsided shorelines. Instead, we found freshwater peat blanketing lowlands, and organic-rich silt and tephra draping higher glacially smoothed bedrock. Basal peat ages place glacier retreat prior to 10.4 ka and imply slowly rising (<0.2 m/ka) relative sea level since ~3.4 ka. Storms rather than tsunamis probably deposited thin, discontinuous deposits in coastal sites. If rupture of the megathrust beneath Simeonof Island produced great earthquakes in the late Holocene, then coseismic uplift or subsidence was too small (≤0.3 m) to perturb the onshore geologic record.

1. Introduction

Global Positioning System (GPS) observations indicate that the megathrust is mostly creeping aseismically beneath the Shumagin Islands. Models of GPS velocities show along-strike variations in the extent of locking on the Aleutian subduction megathrust and suggest that the Shumagin gap is incapable of generating a great earthquake by itself [*Fournier and Freymueller*, 2007]. East of the gap, below the Semidi Islands, their models suggest that the subduction interface is nearly fully locked (90%) (Figure 1). Rupture of this area in 1938 produced a *M*8.2 earthquake that released its greatest moment in the eastern part of the aftershock zone, stopping short of the Shumagin gap [*Johnson and Satake*, 1994]. To the west, *Fournier and Freymueller* [2007] infer that locking decreases to 30% below the Shumagin Islands and is reduced to zero at Sanak Island where the interface appears to be entirely creeping.

Despite GPS evidence of a creeping megathrust, the longer history of great earthquakes in the Shumagin region remains uncertain. Russian accounts of strong shaking and a high tsunami at Three Saints Bay on southwestern Kodiak Island and strong shaking at Unga Island, 400 km southwest of Kodiak (Figure 1b), imply rupture of the megathrust on 21 July 1788 [*Soloviev*, 1990]. Written records also describe tsunami flooding >30 m high on Sanak and Unga Islands that accompanied a second strong earthquake in the Shumagin gap on 6 August 1788 (see Text S1) [*Lander*, 1996]. Although the accounts clearly distinguish two earthquakes in 1788, neither earthquake requires a 400+ km long rupture of the megathrust between Kodiak and the Shumagin Islands because their individual impacts were reported over smaller geographic areas.

Reports of tectonically uplifted marine terraces in the Shumagin Islands have contributed further uncertainty about the size and frequency of past gap-filling earthquakes. The low-relief coastal topography of Simeonof Island resembles the brim of a hat (Figure 1c), distinguishing it from adjacent islands of the Shumagin archipelago with shorelines backed by steep coastal cliffs. Early archeological studies [*Winslow and Johnson*, 1989] interpreted sites of Aleut occupation along the island's brim as evidence for a suite of tectonically uplifted marine terraces that range in age from 2000 to 8000 years old [*Winslow and Johnson*, 1989]. However, our investigation of Simeonof Island found no evidence for uplifted marine terraces. The findings reported in this paper imply that Shumagin gap ruptures capable of launching a potentially destructive tsunami toward

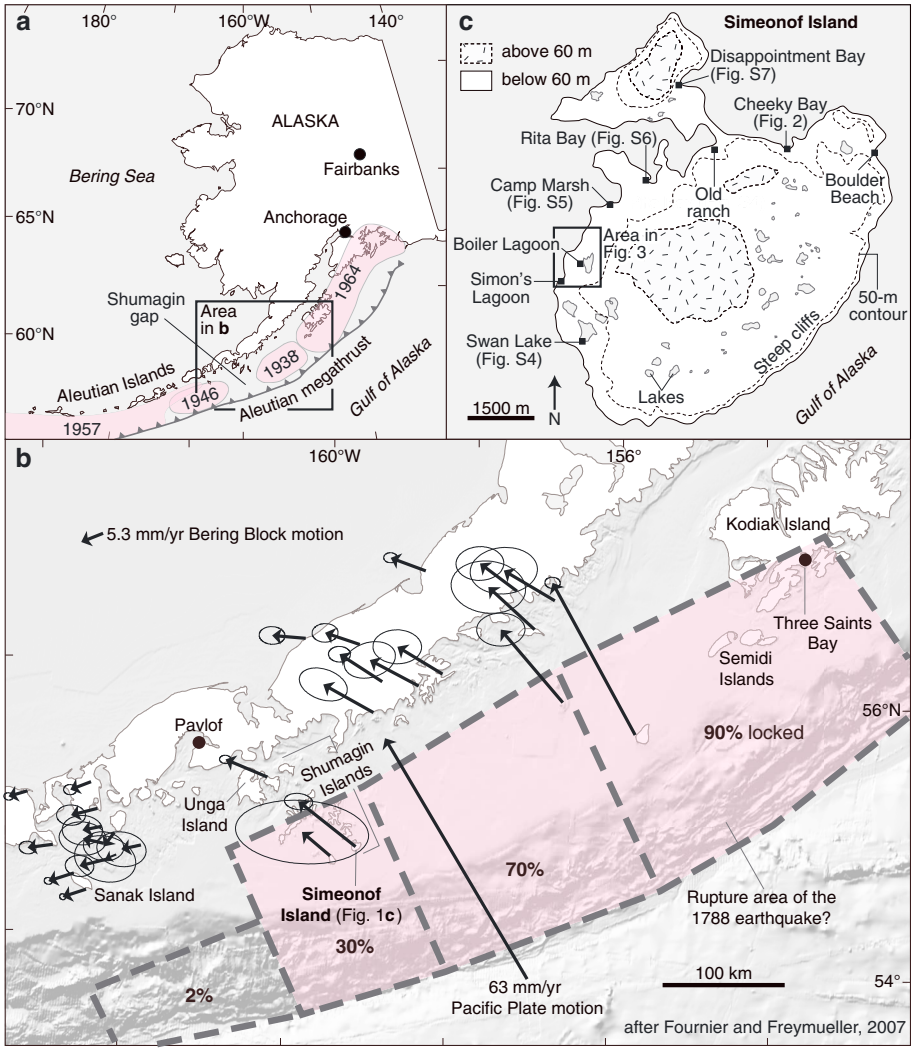

Figure 1. (a) Location of the Shumagin Islands within the plate tectonic setting of the Alaska-Aleutian subduction zone. Rupture areas of historical great earthquakes shown in pink. (b) Velocity field of the Alaska Peninsula and the eastern Aleutian Islands observed by GPS [*Fournier and Freymueller*, 2007]. Surface projections of locked plate interfaces shown by dashed line; numbers depict the percentage of coupling for each fault plane. Inferred rupture area of the 1788 earthquake shown in pink. (c) Simeonof Island, located in the easternmost part of the Shumagin archipelago 120 km from the Aleutian trench, has a hat-like brim of coastal lowlands (<60 m above sea level (asl)) surrounding granitic uplands (>60 m asl). We investigated nine sites along the northwest coast of the island.

the densely populated coasts of Hawaii and southern California [*Butler*, 2012; *Ryan et al*., 2012] have not occurred in the past 3400 years.

2. Approach and Methods

To investigate previously interpreted marine terraces on Simeonof Island, we surveyed 12 shore-normal topographic profiles, examined 10 natural bluff exposures, dug six shallow (<1.5 m deep) soil pits (Figure S1) and assessed the presence or absence of elevated shore platforms and overlying beach deposits. The elevations and horizontal positions of profiles and pits were estimated with real-time kinematic surveys using GPS tied to a local tidal datum. A water-level logger, deployed in a protected bay on the northwestern side of the island (Camp Marsh in Figure 1c), measured local tides at 5 min intervals. Observed tidal time series and local tidal datums were validated against verified tides at the nearest NOAA tide gage (9459450) at Sand Point and a numerical model of tide predictions at Simeonof Island (see *Kemp et al*. [2013] and supporting information (Text S2 and Figure S2) for details).

Seeking evidence for great earthquakes and tsunamis that may have struck the island in the past, we searched for tsunami deposits and stratigraphic signs of coseismic displacement (uplift or subsidence) in coastal sediment. We examined deposits exposed in coastal bluffs, beneath intertidal wetlands, and freshwater coastal bogs 2–5 m above mean sea level and within the reach of high tsunamis. Exploratory tools included 2.5 to 5 cm wide, handheld gouge corers, Russian peat augers, and spades. Paleoseismic studies at other subduction zones reconstruct records of past great earthquakes by documenting coastal geologic evidence for sudden tectonic uplift, subsidence, and tsunami inundation [e.g., *Nelson and Manley*, 1992; *Melnick et al*., 2006; *Satake and Atwater*, 2007; *Sawai et al*., 2012]. Sea-level indicators, including salt marsh plant communities, fossil marine diatoms, lithostratigraphic relations, and sediment geochemistry (stable carbon isotopes), distinguished sediment deposited below the mean high water (MHW) tidal datum from sediment deposited above the datum.

Finally, we used an elastic dislocation model to explore the megathrust parameters necessary to predict ~0.3 m of subsidence or uplift on Simeonof Island (see Text S3 for explanation of methods). Land-level changes greater than 0.3 m should produce more easily identified and longer lasting evidence, commonly expressed as sharp contacts in coastal sediments as demonstrated by coastal paleoseismic studies above other subduction zones [e.g., *Hamilton and Shennan*, 2005; *Nelson et al*., 2008]. We use the 0.3 m displacement estimate from modeling to constrain the maximum magnitude of past earthquakes that might not produce detectable lithostratigraphic or geomorphic evidence in the geologic record.

3. Absence of Uplifted Marine Terraces

Simeonof Island's low-relief coastal perimeter and glacial landforms led earlier workers to interpret a history of tectonic uplift for which we find no evidence. *Grantz and Cobb* [1968] called the island an erosional remnant jutting above the extensive Shumagin-Kodiak Shelf. Surrounding two bedrock hills formed of biotite-granodiorite, peat-forming freshwater bogs (muskeg) form a low-relief surface dotted by lakes. Tectonic strain has tilted the surface arcward [*Beavan*, 1994], exposing 50 m high sea cliffs on the Pacific side that give way to lowlands surrounding lagoons and protected harbors on the island's leeward, northwest side (Figure 1c). *Grantz and Cobb* [1968] speculated that the surface was underlain by a few meters of beach and windblown sand and glacial deposits overlying a "wave-cut platform" of undetermined age. Later, archeological reports claimed that tectonically uplifted marine terraces on the Shumagin Islands, including Simeonof Island, recorded a history of frequent earthquakes with vertical displacements large enough to drive changes in Aleut occupation [*Winslow and Johnson*, 1989]. Our observations suggest a different tectonic history.

Three lines of reasoning cast doubt on the hypothesis that flights of tectonically uplifted marine terraces comprise the island's coastal brim. The first comes from radiocarbon ages from basal organic-rich sediment near present sea level that constrain the retreat of glaciers to before 10.4 ka (Figure 2). The organic-rich sediment, which probably formed in an upland muskeg environment, overlies dense sand and gravel that we interpret as till. Similar muskeg environments occur along the island's lowlands above the highest tides. Three radiocarbon dates on detrital wood and fossil insects (*Coleoptera*) in the organic-rich sediment range from 7.0 to 10.7 ka (Table S1) and attest to early Holocene formation of upland muskeg deposits, now near present sea level, ruling out later glacioisostatic or tectonic uplift of the coast. Our mapping of the island's brim is consistent with reconstructions of glaciers extending from the Alaska Peninsula to the outer edge of the continental shelf during the last glacial maximum, which ended about 14.7 ka [*Mann and Peteet*, 1994].

A second problem with the uplifted-terrace hypothesis is the conspicuous absence of coincident marine strandlines, now established by detailed GPS leveling along more than 10 km of coast. Faint tonal lineaments, slope breaks, linear ridges, and sidehill benches are apparent in satellite imagery of Simeonof Island (Figure S1a). However, topographic profiles show few terrace-like landforms with coincident elevations (Figure S1b) that extend beyond local catchments. Instead, the profiles reveal an absence of extensive, step-like marine terraces along the coast, unlike the tectonically uplifted terraces and strandlines along other subduction zone coasts [*Plafker and Rubin*, 1978; *Ota and Yamaguchi*, 2004; *Melnick et al*., 2006]. Furthermore, marine deposits were absent in all exposures of coastal bluffs (Figure S3) and soil pits that we examined. The simplest interpretation for the discontinuous topographic lineaments on Simeonof Island is that these landforms are related to glacial erosion and deposition.

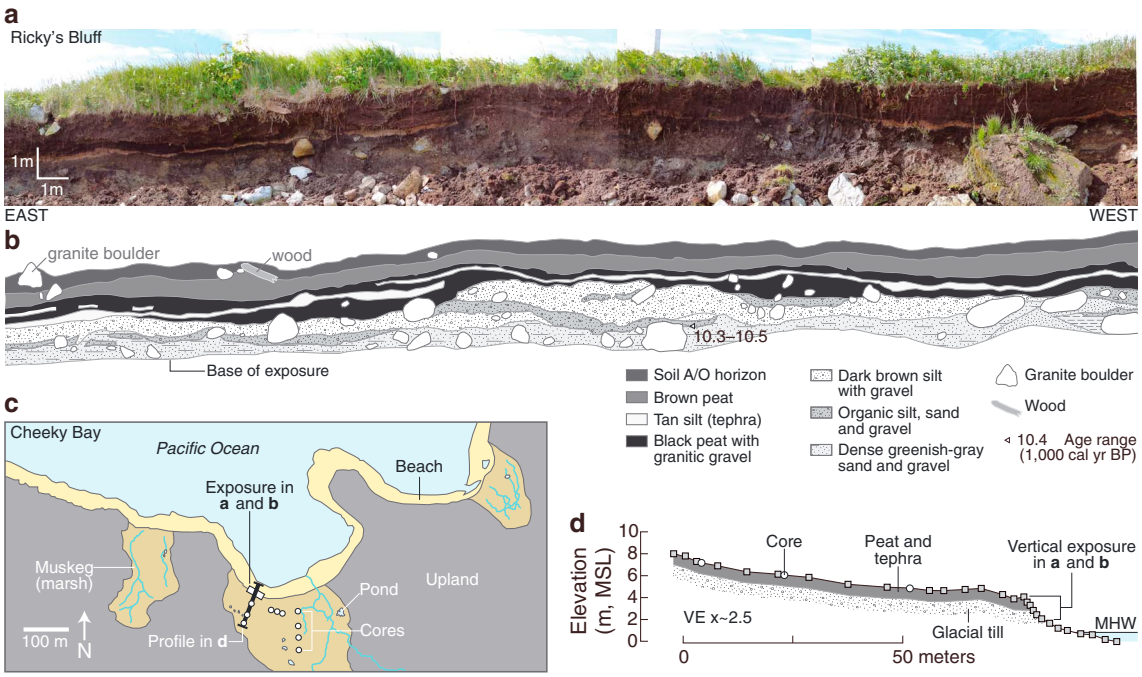

Figure 2. (a) Photomosaic and (b) log of muskeg peat overlying glacial deposits exposed in a coastal bluff at Cheeky Bay. An age of 10.3–10.5 ka from the base of peat exposed in the outcrop provides an upper limit on the time of ice retreat at the end of the last glaciation. (c) We used cores to investigate sediment beneath muskeg environments inland from the bluff. (d) Profile at Cheeky Bay showing an absence of marine deposits in cores and bluff exposures, which imply that relative sea level has been lower than the present shoreline over the entire Holocene.

A third line of evidence against a rapidly uplifting coast is the observation that soil profiles in outcrops and hand-dug pits show uniform soil development across the island. If Simeonof Island had been repeatedly raised by coseismic uplift, higher surfaces should show greater soil profile development. Instead, on all surfaces regardless of elevation we observed cumulic soils developed in silt deposited on deeply weathered granodiorite and over thin (<1 m thick), surficial deposits interpreted as till (Figure S3). Radiocarbon ages from weakly developed soil horizons (Bw) of similar thickness (Figure S1c) suggest a postglacial landscape mantled by tephras into which are developed soils of similar relative age.

4. Shoreline Change and Slow Relative Sea-Level Rise

Numerous abandoned shorelines surround lakes and lagoons along the island's coast, but we found no evidence that these are marine in origin (Figures S4–S6). Because the shorelines are restricted to local lake basins and small coastal embayments, we interpret them as evidence for fluctuating water levels in interconnected coastal hydrological systems rather than sudden, earthquake-related relative sea-level (RSL) changes. Where interconnected chains of lakes intersect the coast, successive shorelines appear to record fluctuating lake levels confined to a local basin. At some sites, gradual RSL rise in the late Holocene led to marine invasion of a lake and further modification of its shorelines.

The best example of marine invasion of a lake comes from the west side of the island at Boiler Lagoon (Figure 3) where a complex of barrier bars and spits formed by ocean waves indicate coastal retreat of the shoreline and subsequent shoreface adjustment on an accreting beach. We infer that the abandoned shorelines surrounding the lagoon reflect lacustrine rather than marine processes because the shorelines do not correlate between adjacent, but hydrologically disconnected basins (Figure S1). Presently, ebb- and flood-tide deltas at either end of the bay's outlet creek demonstrate clear tidal influence. Intriguing lobate sand ridges near the outlet of Boiler Lagoon (profile BB-4, Figure 3c) may reflect an earlier flood-tide delta [e.g., *Morton et al.*, 2000] that formed when the former lake was first breached by the sea. Marine invasion probably occurred before 2.0–2.3 ka, based on basal peat ages (Table S1) from a stratigraphic transect at Boiler Lagoon. The transect shows interbedded sand and peat

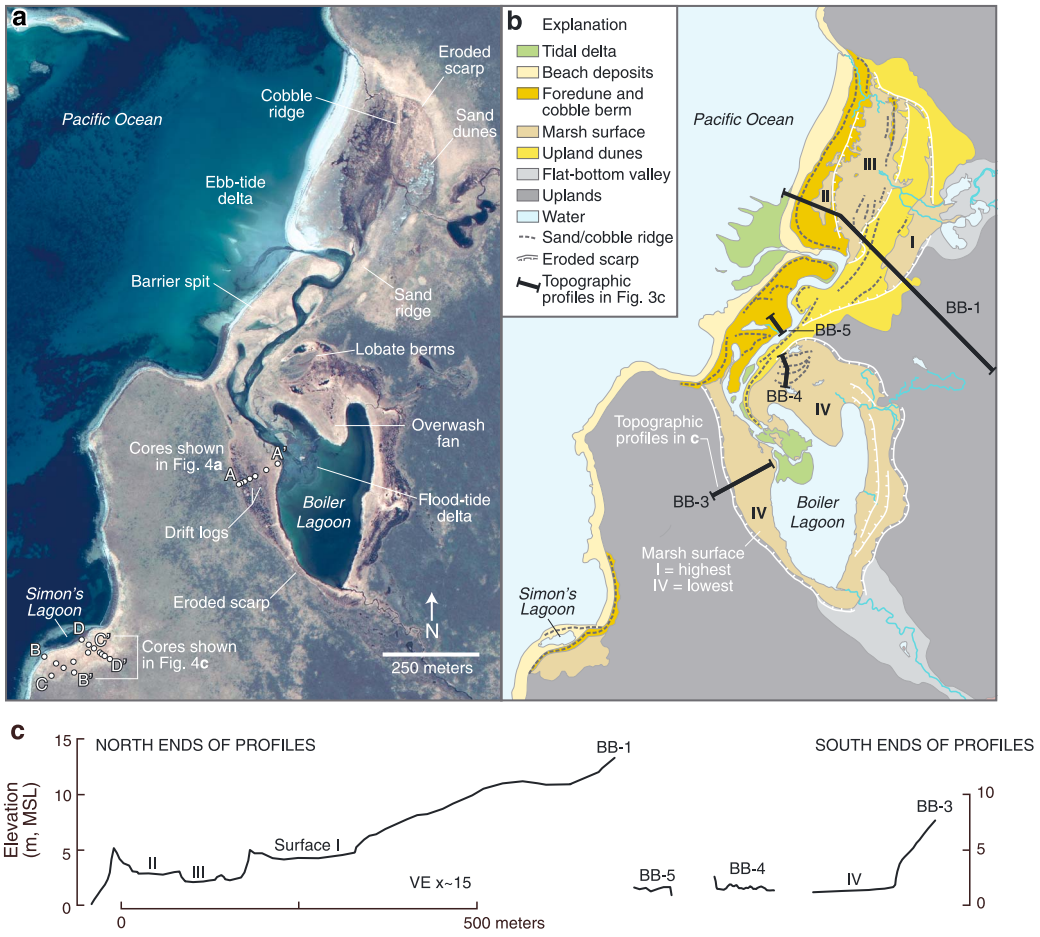

Figure 3. (a) Satellite image of the Boiler Lagoon and Simon's Lagoon field sites. Stratigraphic profiles of cores plotted on image are shown in Figure 4. (b) Map of surficial deposits and geomorphological features surrounding Boiler Lagoon. (c) Topographic profiles, plotted above, show four marsh surfaces at different elevation (indicated by Roman numerals). Constructional ridges and abandoned shorelines reflect marine invasion of a coastal lake and subsequent adjustments of the beach shoreface.

at a depth of ~1 m (Figure 4), which suggests a gradual shift from a sandy intertidal environment to a peat-forming high marsh similar to the present environment [*Kemp et al.*, 2013].

To reconstruct RSL change, we relied on a number of qualitative sea-level indicators that relate the elevation of coastal environments to mean high water (MHW), a local tidal datum at 0.81 m above mean sea level (MSL) (Figure S2b). First, the core transect at Boiler Lagoon (Figure 4a) crossed a salt marsh colonized by *Elymus mollis*, *Carex* spp., and *Potentillia egedei*—all peat-forming, high-marsh plant species usually found above MHW [*Kemp et al.*, 2013]. Second, we observed dead and decaying marine algae that formed conspicuous wrack line deposits near MHW on the modern beach and along the shoreline of Boiler Lagoon. Finally, beach and lagoon sand dominated sedimentary environments below MHW.

Variations in $\delta^{13}C$ values of bulk sediment samples from a core at Boiler Lagoon (Table S2) distinguish sediment deposited in marine versus high-marsh environments and support estimates of paleoelevation relative to MHW. Bulk samples of peat from the Boiler Lagoon core (Figure 4b) have $\delta^{13}C$ values that range from −27.4‰ to −25.7‰, including an analysis of surface peat (−26.9‰). The range in $\delta^{13}C$ for these peat samples is similar to $\delta^{13}C$ for surface sediment from middle– to high– salt marsh environments (−27.3 ± 1.4‰) at Siletz Bay, Oregon [*Engelhart et al.*, 2013]. Bulk samples of sandy sediment stratigraphically below the peat have much higher $\delta^{13}C$ values (−17.2‰ to −21.0‰), which are consistent with $\delta^{13}C$ values ranging from −23‰ to −18‰ for marine and open coastal sediments [*Hedges and Mann*, 1979; *Wilson et al.*, 2005]. The modern vegetation on Simeonof Island lacks C4 species with high $\delta^{13}C$ values (e.g., *Distichlis spicata*).

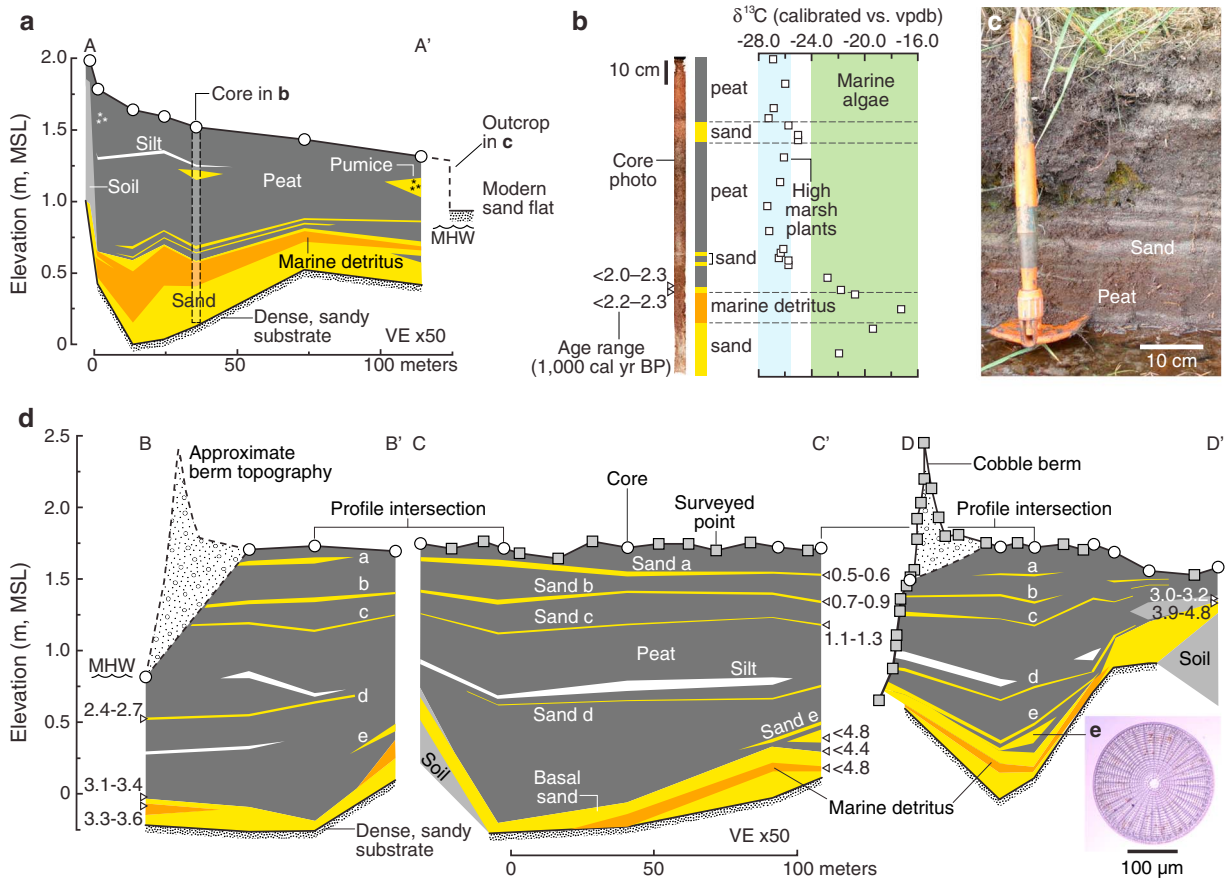

Figure 4. (a) Stratigraphic profile of sediment beneath a marsh at Boiler Lagoon (A—A′ in Figure 3b). (b) Variations in $\delta^{13}C$ values in the sediment samples show a change from sandy marine environment to a high-marsh peat-forming environment. (c) Discontinuous sand layers interbedded with peat attest to frequent marine inundation of the marsh during extreme tides and unusual storms. (d) Stratigraphic profile of sediment beneath the marsh at Simon's Lagoon. (e) Fossils of *Arachnoidiscus japonicas*, a large (250 µm diameter) centric diatom that attaches to seaweed, were present in sandy and peaty sediment and implying marine influence.

Analyses of organic-rich detritus interbedded in the sand yielded the highest $\delta^{13}C$ value (−17.2‰), which may indicate contributions of marine algae (−16‰ to −24‰) or sea grasses (marine C4 plant; −14‰ to −19‰) [*Deines*, 1980; *Tyson*, 1995]. The organic-rich detritus probably was deposited in a sandy environment near or just below MHW much like the algal debris observed along the modern wrack line. Because the overlying peaty sediment reflects a high-marsh environment above MHW, we infer that the elevations of peat-over-sand contacts in sediment cores are a reasonable upper limit for former elevations of MHW.

Constraints on former tide levels and the time of the transition between sandy marine and high-marsh peat environments in cores from Simon's Lagoon allowed us to reconstruct late Holocene RSL change at Simeonof Island. Like the Boiler Lagoon transect, 12 cores at Simon's Lagoon revealed a stratigraphy of marine sand overlain by high-marsh peat (Figure 4d). Seeds of *Hippurus vulgaris*, an aquatic perennial herb [*Hultén*, 1968], sampled above and below the peat-over-sand contact (cores SL-01A and C) provided bracketing ages that place the shift in depositional environment between 3.1 and 3.6 ka (Table S1). Because the present-day wrack line of marine detritus on the ocean beach and along the shoreline of Boiler Lagoon occurs near MHW, as determined by tidal modeling [*Kemp et al.*, 2013], the marine detritus found in sandy sediment beneath Simon's Lagoon provides a reasonable lower limit for the former elevation of MHW. The base of peat overlying the sandy sediment provides a reasonable upper bound on the elevation of paleo-MHW because the peat contains seeds of *H. vulgaris* common in fresh-brackish coastal wetlands in Alaska. The depths and age ranges of *H. vulgaris* seeds that bracket the basal peat contact (Table S1) indicate that RSL has risen very slowly at a rate of ~0.2 mm/yr since 3.1 to 3.6 ka. The relative stability of sea level in the late Holocene and the lack of evidence for high tsunamis or other sudden changes in sea level suggest that large tectonic displacements have not perturbed Simeonof Island in the past few millennia.

5. Absence of Evidence for Great Earthquakes and High Tsunamis

We found no stratigraphic or geomorphic evidence for sudden RSL changes along the coast of Simeonof Island that requires explanation as vertical displacement caused by megathrust slip directly beneath the island. Intriguingly, coastal sediment beneath Boiler Lagoon and Simon's Lagoon lack stratigraphic evidence for sudden RSL changes—either up or down—that have provided clues of sudden tectonic displacement accompanying earthquakes at other subduction zones [e.g., *Melnick et al*., 2006; *Satake and Atwater*, 2007]. Instead, cores that exposed interbedded sand and peat revealed a history of gradual shoaling of coastal lagoons during very slow RSL rise in the late Holocene, uninterrupted by sudden tectonic displacement.

Coastal sites on Simeonof Island lack extensive sand sheets consistent with deposition by high tsunamis. Beneath some marshes the stratigraphy includes thin (0.5 to 3 cm), often discontinuous sheets of sandy sediment interrupting homogeneous intervals of peat (Figure 4c). Compositions of sand layers are similar to the granitic composition of beach sand suggesting a marine source. At Simon's Lagoon, five or six sheets of granitic sand interbedded with peat suggest marine water invaded the marsh on average every 480 to 760 years (Figure 4d and Table S1). However, coring on uplands above the marsh demonstrated that sand dispersal was limited to local basins below the highest tides, which casts doubt on high tsunamis as an explanation. Drift logs scattered across marsh surfaces and the relatively low elevation of the deposits within the intertidal zone make extreme tides, reconfigurations of sand barriers, or large storms equally reasonable explanations for sand deposition but do not rule out low-amplitude tsunamis. Even sites on the eastern side of the island facing the trench (Disappointment Bay, Figure S7; and Boulder Beach, Figure 1c) lacked clear evidence for tsunami inundation.

We used an elastic model to generate scenarios of megathrust rupture beneath Simeonof Island that would produce uplift or subsidence of 0.3 m or less for a range of updip and downdip rupture limits. The scenarios predict maximum estimates of slip and correspondingly small (≤0.3 m) vertical displacements consistent with the lack of detectable lithostratigraphic or geomorphic evidence on Simeonof Island. Scenarios that entail slip extending from the trench to a range of depths (20–35 km) require 1.8–5 m of fault slip to produce ≤ 0.3 m of subsidence unlikely to be detected in coastal sediment (Figure S8a and Table S3). Other scenarios, where rupture stops short of the trench at depths between 15 and 25 km, produce ≤0.3 m of vertical displacement of the island for modeled slip below 2–4 m (Figure S8b). The predicted maximum slip decreases in scenarios that place the subsidence axis closer to the island. The rupture scenario from 40 km depth to the trench places the hingeline near Simeonof Island, which allows a much larger earthquake with 15 m of slip on the megathrust—an outsized scenario that predicts too little vertical displacement to leave lasting evidence in coastal sediment (Figure S8a).

6. Discussion

The lack of evidence for recent great earthquakes and high tsunamis on Simeonof Island must be reconciled with accounts in 1788 of strong shaking and severe tsunami flooding in the Shumagin region (Text S1). If a single great earthquake in 1788 ruptured from Sanak Island to Kodiak Island across the Shumagin gap, then evidence for detectible surface displacement and tsunami inundation should be preserved at coastal sites like those we investigated on Simeonof Island. An outsized rupture scenario where 15 m of uniform slip extends to 40 km depth (Figure S8) could explain a gap-filling rupture in 1788. Scaling relations between average slip and seismic moment for historical great earthquakes suggest that the outsized rupture scenario is equivalent to an earthquake with $M > 9$ [*Murotani et al*., 2013]. Because this scenario locates the hingeline near Simeonof Island, the uplift predicted by elastic modeling would be too low to produce a lasting signature in coastal deposits. However, large seafloor displacements modeled for this scenario would generate a high tsunami, for which we find no evidence. A giant Shumagin rupture scenario predicts another result that could be verified by geological evidence—substantial coseismic subsidence of the Shumagin archipelago arcward of Simeonof Island, which could be investigated by future fieldwork. Until such evidence is found, a giant Shumagin scenario does not satisfactorily explain a >400 km long rupture in 1788.

An alternative hypothesis involving two large earthquakes that occurred separately on 21 July and 6 August 1788 [*Lander*, 1996] is more consistent with our findings. Russian accounts indicate that each earthquake generated locally high tsunamis [*Soloviev*, 1990], but their inundation is not apparent in the sedimentary record of Simeonof Island. Our elastic modeling suggests that if slip on the megathrust occurred on the

segment beneath Simeonof Island, then it probably did not exceed 5 m (Figure S8). The resulting surface deformations in these scenarios predict <0.3 m of subsidence of the island and insufficient RSL change to produce lasting geologic evidence. If the scenarios involve 125 km long ruptures of the eastern Shumagin gap, then *M*7.7–*M*8.1 represent upper limits on magnitudes (Table S3). Longer ruptures involving the Shumagin gap could produce higher magnitude earthquakes, but substantial slip would likely occur on adjacent segments. Models of interseismic deformation at Simeonof Island for 8 of the 10 rupture scenarios predict horizontal displacements consistent with modern GPS velocities assuming a 30–100% locked megathrust (Figures S8c–S8f and Text S3).

Finally, the lack of geologic evidence for great earthquakes and tsunamis on Simeonof Island implies that a substantial component of plate convergence along the Shumagin segment has been accommodated by aseismic slip over the past 3400 years. If so, large earthquakes like the historical *M*7–*M*7.5 shocks of the twentieth century (Figure S9) may be sufficient to release the elastic strain stored in the Shumagin gap [*Estabrook and Boyd*, 1992; *Fournier and Freymueller*, 2007]. Evidence supporting this view includes deformation observed during the 1993 *M*6.9 Shumagin earthquake, which uplifted Simeonof Island relative to Sand Point by ~0.03 m [*Beavan*, 1994] and produced too little vertical deformation to create easily identifiable and long-lasting geologic evidence. Moreover, the Sand Point tide gage and ocean bottom pressure sensors within 300 km of the 1993 Shumagin earthquake failed to detect the small-amplitude tsunami the earthquake generated [*Tanioka et al.*, 1994]. If low tsunamis like those produced by the 1993 earthquake transported sand into coastal settings, the deposits would be indistinguishable from sand deposited by storm waves, reconfiguration of the shoreline, or extreme tides. The absence of evidence for vertical tectonic displacement in coastal sediment of Simeonof Island is consistent with strain release during large (*M*7–*M*8) earthquakes and a component of aseismic slip. In the Shumagin gap, it appears that aseismic slip may have been a persistent mode of subduction in late Holocene time.

Acknowledgments

The U.S. Geological Survey's seismic and tsunami hazards projects supported this research. D. Peteet identified fossil seeds submitted for radiocarbon analysis, and E. Hemphill-Haley identified marine diatoms. A. Bender, L. Munk, and K. Wallace assisted with radiocarbon and geochemical sample preparation. M. Rogers performed geochemical analyses. We thank P. Haeussler for his insightful contributions throughout the project. Reviews by A. Nelson, Jeff Freymueller, and Chris Goldfinger improved the paper. R.C.W. prepared the manuscript and participated in field investigations with R.W.B., S.E.E., G.G., and R.D.K., listed alphabetically. W.D.B. contributed elastic dislocation modeling data.

The Editor thanks Jeffrey Freymueller and Chris Goldfinger for their assistance in evaluating this paper.

References

Beavan, J. (1994), Crustal deformation measurements in the Shumagin seismic gap, Alaska, U.S. Geol. Surv. Open-File Rep. 94-176, pp. 195–205.

Butler, R. (2012), Re-examination of the potential for great earthquakes along the Aleutian Island Arc with implications for tsunamis in Hawaii, *Seismol. Res. Lett.*, *83*(1), 29–38, doi:10.1785/gssrl.83.1.29.

Deines, P. (1980), The isotopic composition of reduced organic carbon, in *Handbook of Environmental Isotope Geochemistry*, edited by P. Fritz and J. C. Fontes, pp. 329–426, Elsevier, Amsterdam.

Engelhart, S. E., B. P. Horton, C. H. Vane, A. R. Nelson, R. C. Witter, S. R. Brody, and A. D. Hawkes (2013), Modern foraminifera, $\delta^{13}C$, and bulk geochemistry of central Oregon tidal marshes and their application in paleoseismology, *Palaeogeogr. Palaeoclimatol. Palaeoecol.*, *377*, 13–27, doi:10.1016/j.palaeo.2013.02.032.

Estabrook, C. H., and T. M. Boyd (1992), The Shumagin Islands, Alaska, earthquake of 31 May 1917, *Bull. Seismol. Soc. Am.*, *82*(2), 755–773.

Fournier, T. J., and J. T. Freymueller (2007), Transition from locked to creeping subduction in the Shumagin region, Alaska, *Geophys. Res. Lett.*, *34*, L06303, doi:10.1029/2006GL029073.

Grantz, A., and E. H. Cobb (1968), Simeonof and Semidi National Wildlife Refuges, in *Summary Report on the Geology and Mineral Resources of the Bering Sea, Bogoslof, Simeonof, Semidi, Tuxedni, St. Lazaria, Hazy Islands, and Forrester Island National Wildlife Refuges Alaska*, U.S. Geol. Surv. Bull., 1260-K, edited by E. H. Cobb et al., pp. 8–13, U.S. Government Printing Office, Washington, D. C.

Hamilton, S., and I. Shennan (2005), Late Holocene relative sea-level changes and the earthquake deformation cycle around upper Cook Inlet, Alaska, *Quat. Sci. Rev.*, *24*(12–13), 1479–1498, doi:10.1016/j.quascirev.2004.11.003.

Hedges, J. I., and D. C. Mann (1979), The lignin geochemistry of marine sediments from the southern Washington coast, *Geochim. Cosmochim. Acta*, *43*, 1809–1818.

Hultén, E. (1968), *Flora of Alaska and Neighboring Territories: A Manual of the Vascular Plants*, pp. 1032, Stanford Univ. Press, Stanford, Calif.

Johnson, J. M., and K. Satake (1994), Rupture extent of the 1938 Alaskan earthquake as inferred from tsunami waveforms, *Geophys. Res. Lett.*, *21*(8), 733–736.

Kemp, A. C., S. E. Engelhart, S. J. Culver, A. R. Nelson, R. Briggs, and P. J. Haeussler (2013), Modern salt-marsh and tidal-flat foraminifera from Sitkinak and Simeonof Islands, southwestern Alaska, *J. Foraminiferal Res.*, *43*, 88–98.

Lander, J. F. (1996), *Tsunamis Affecting Alaska 1737–1996*, 195 pp., NOAA/NGDC, Boulder, Colo.

Mann, D. H., and D. M. Peteet (1994), Extent and timing of the last glacial maximum in southwest Alaska, *Quat. Res.*, *42*, 136–148.

Melnick, D., B. Bookhagen, H. P. Echtler, and M. R. Strecker (2006), Coastal deformation and great subduction earthquakes, Isla Santa Maria, Chile (37 S), *Geol. Soc. Am. Bull.*, *118*(11–12), 1463–1480, doi:10.1130/B25865.1.

Morton, R. A., J. G. Paine, and M. D. Blum (2000), Responses of stable bay-margin and barrier-island systems to Holocene sea-level highstands, western Gulf of Mexico, *J. Sediment. Res.*, *70*(3), 478–490.

Murotani, S., K. Satake, and Y. Fuji (2013), Scaling relations of seismic moment, rupture area, average slip, and asperity size for M~9 subduction-zone earthquakes, *Geophys. Res. Lett.*, *40*, 5070–5074, doi:10.1002/grl.50976.

Nelson, A. R., and W. F. Manley (1992), Holocene coseismic and aseismic uplift of Isla Mocha, south-central Chile, *Quat. Int.*, *15*, 61–76.

Nelson, A. R., Y. Sawai, A. E. Jennings, L.-A. Bradley, L. Gerson, B. L. Sherrod, J. Sabean, and B. P. Horton (2008), Great-earthquake paleogeodesy and tsunamis of the past 2000 years at Alsea Bay, central Oregon coast, U.S.A., *Quat. Sci. Rev.*, *27*(7–8), 747–768, doi:10.1016/j.quascirev.2008.01.001.

Ota, Y., and M. Yamaguchi (2004), Holocene coastal uplift in the western Pacific Rim in the context of Late Quaternary uplift, *Quat. Int.*, *120*, 105–117.

Plafker, G., and M. Rubin (1978), Uplift history and earthquake recurrence as deduced from marine terraces on Middleton Island, Alaska, in *Proceedings of Conference VI, Methodology for Identifying Seismic Gaps and Soon-to-Break Gaps*, U.S. Geological Survey Open-File Report 78-943, pp. 687–721.

Ryan, H. F., R. von Huene, R. E. Wells, D. W. Scholl, S. Kirby, and A. E. Draut (2012), History of earthquakes and tsunamis along the eastern Aleutian-Alaska megathrust, with implications for tsunami hazards in the California Continental Borderland, in *Studies by the U.S. Geological Survey in Alaska, 2011*, U.S. Geological Survey Professional Paper 1795–A, edited by J. A. Dumoulin and C. Dusel-Bacon, 31 p., U.S. Geological Survey, Reston, Va.

Satake, K., and B. F. Atwater (2007), Long-term perspectives on giant earthquakes and tsunamis at subduction zones, *Annu. Rev. Earth Planet. Sci.*, *35*(1), 349–374, doi:10.1146/annurev.earth.35.031306.140302.

Sawai, Y., Y. Namegaya, Y. Okamura, K. Satake, and M. Shishikura (2012), Challenges of anticipating the 2011 Tohoku earthquake and tsunami using coastal geology, *Geophys. Res. Lett.*, *39*, L21309, doi:10.1029/2012GL053692.

Soloviev, S. L. (1990), Sanak–Kodiak tsunami of 1788, *Sci. Tsunami Hazards*, *8*(1), 34–38.

Tanioka, Y., K. Satake, L. Ruff, and F. González (1994), Fault parameters and tsunami excitation of the May 13, 1993, Shumagin Islands earthquake, *Geophys. Res. Lett.*, *21*(11), 967–970.

Tyson, R. V. (1995), *Sedimentary Organic Matter: Organic Facies and Palynofacies*, Chapman & Hall, London.

Wilson, G. P., A. L. Lamb, M. J. Leng, S. Gonzalez, and D. Huddart (2005), δ13C and C/N as potential coastal palaeoenvironmental indicators in the Meresy Estuary, U. K., *Quat. Sci. Rev.*, *24*, 2015–2029.

Winslow, M. A., and L. L. Johnson (1989), Prehistoric human settlement patterns in a tectonically unstable environment: Outer Shumagin Islands, southwestern Alaska, *Geoarchaeology*, *4*(4), 297–318.